Smart Structures and Systems, *Vol. 27, No. 5 (2021) 861-870*
DOI: https://doi.org/10.12989/sss.2021.27.5.861

Subgrade assessment using automated dynamic cone penetrometer to manage geo-infrastructures

Sang Yeob Kim [1a], Jong-Sub Lee [2b] and Won-Taek Hong*[3]

[1] *Department of Civil and Environmental Engineering, University of Illinois at Urbana-Champaign, 205 North Mathews Avenue, Urbana, IL 61801, USA*
[2] *School of Civil, Environmental and Architectural Engineering, Korea University, 145 Anam-ro, Seongbuk-gu, Seoul 02841, Republic of Korea*
[3] *Department of Civil & Environmental Engineering, Gachon University, 1342 Seongnam-daero, Sujeong-gu, Seongnam-si, Gyeonggi-do 13120, Republic of Korea*

(*Received September 3, 2020, Revised March 5, 2021, Accepted March 24, 2020*)

Abstract. For the efficient management of geo-infrastructures in the field, engineering properties of the subgrade should be reliably and rapidly investigated. The objective of this study is to estimate and compare the strength and stiffness parameters of subgrades using portable in-situ devices. An automated dynamic cone penetrometer (ACP), dynamic cone penetrometer (DCP), and light falling weight deflectometer (LFWD) are adopted and applied at nine points of soft ground in South Korea. The N-value from the ACP (N_{ACP}), which efficiently assesses the relatively deep subgrade, is correlated with the dynamic cone penetration index (DCPI) and dynamic deflection modulus (E_{vd}). Test results show that the DCPI and E_{vd} can be estimated in terms of N_{ACP}. In particular, the relationship between E_{vd} and N_{ACP} is improved when the strain influence factor of the target ground is considered. For the assessment of strength and stiffness parameters, the California bearing ratio (CBR), relative density (D_r), internal friction angle (ϕ), and elastic moduli determined by the plate loading test (PLT), soil stiffness gauge (SSG), falling weight deflectometer (FWD) are estimated using N_{ACP}. The ACP test with the relationships between engineering parameters and N_{ACP} may be an effectively method to assess the overall characteristics of the subgrade.

Keywords: automated dynamic cone penetrometer (ACP); dynamic cone penetrometer (DCP); engineering parameter; light falling weight deflectometer (LFWD); subgrade

1. Introduction

The mechanical properties (e.g., strength and stiffness) of subgrades have been evaluated in both the laboratory and the field to obtain engineering parameters for the safety design and effective management of geo-infrastructures (Farghaly 2015). In the laboratory, however, it is extremely difficult to obtain an impeccably undisturbed sample whose structure completely remains in situ (Mohammadi *et al*. 2008). In addition, laboratory tests do not sufficiently predict the mechanical degradation of subgrade materials due to compaction during construction and repetitive loading during the operation of geo-infrastructures (Gidigasu 1980). In the field, conventional in-situ tests such as the standard penetration test (SPT) and cone penetration test (CPT) have been widely conducted (Mir *et al*. 2017, Kong *et al*. 2018). However, the heavy equipment in conventional in-situ devices has limited applicability in areas with low accessibility (Kim and Lee 2020). To address this limitation, a number of portable in-situ devices have been developed for quantitative evaluations of the mechanical properties in the field (Alshibli *et al*. 2005, Sawangsuriya and Edil 2005, Byun and Lee 2013, Byun and Kim 2020, Lee and Byun 2020).

Light falling weight deflectometers (LFWD) have been widely used in the field for the assessment of subgrade stiffness. The LFWD is efficient in monitoring the stiffness variation and assessing the quality of compaction during construction, because it offers advantages of fast testing and quantitative evaluation (Lee *et al*. 2014). In particular, the LFWD is suitable for evaluating the stiffness of subgrades underneath railway and roadway pavements because the dynamic deflection modulus (E_{vd}) is measured by applying dynamic loads. Meanwhile, the California bearing ratio (CBR), which represents the strength, is regarded as the most convenient and reliable criterion to evaluate the bearing capacity of soils (Roy 2016). The CBR test is applicable in the field because of its simplicity and capability of rapid measurements for subgrade strength without excavation (Harison 1989). Furthermore, CBR has been employed for the design of flexible pavements on the basis of correlations with a number of other engineering parameters (Usluogullari and Vipulanandan 2011, Putri *et al*. 2012, Sujatha *et al*. 2018). Despite the advantages of the LFWD and CBR tests, field application is only recommended for a certain shallow depth owing to the limited effective depth, which is twice the diameter of the

*Corresponding author, Ph.D., Assistant Professor,
E-mail: wthong@gachon.ac.kr
[a] Ph.D., Postdoctoral Research Associate
[b] Ph.D., Professor

ISSN: 1738-1584 (Print), 1738-1991 (Online)

loading plate for LFWD (Nazzal *et al*. 2004) and a depth less than 1 m, which is similar to the influence depth of a vehicle load, for CBR (Briaud 2013). Further, the strain influence factor that varies along the depth must be considered to analyze the measured representative mechanical properties.

One of the most applicable in-situ devices for subgrade characterization is a dynamic cone penetrometer (DCP); hence, the DCP has been used for pavement design using correlations with LFWD and CBR (Gabr *et al*. 2000, Chen *et al*. 2005, George *et al*. 2009). The DCP is portable, and its test procedure is simple and convenient for obtaining a continuous subgrade profile (Hong *et al*. 2016). The remarkable advantage of the DCP is that the dynamic cone penetration index (DCPI), whose unit is the penetration depth per blow, represents the strength for each measured depth. Thus, the consideration of the strain influence factor with respect to depth, which is recommended for the evaluation of mechanical properties using LFWD and CBR, is not necessary. However, manual hammer blowing and measuring each DCPI individually extends the test duration, and the small difference in diameters of the driving rod and the cone tip generates frictions between the ground and the driving rod, which causes the loss of driving energy. Thus, the total penetration depth of the DCP is typically 2–3 m. In contrast, an automated dynamic cone penetrometer (ACP) equipped with an automatic hammer system is applied for subgrade assessments by measuring blow counts per 100 mm, which is the inverse concept of unit for DCPI. The automatic hammer system and measuring unit concept shortens the time required for the in-situ test, as compared to the DCP test. Furthermore, the impact energy of ACP with a 294.3 N hammer and the 200 mm drop height, which is greater than that of the DCP with a 78.5 N hammer and a 575 mm drop height, provide a deeper test depth.

The objective of this study is to evaluate the strength and stiffness of a subgrade using portable in-situ devices and compare the measured mechanical properties. First, this study introduces the specifications and testing procedures of ACP, DCP, and LFWD. Thereafter, the in-situ test results of nine points are presented by the N-value (N_{ACP}) from the ACP, DCPI from the DCP, and dynamic deflection modulus (E_{vd}) from the LFWD. Finally, N_{ACP} is correlated with DCPI and E_{vd}, considering the strain influence factor to verify the adaptability of ACP. In addition, the relationships of N_{ACP} with the strength and stiffness parameters of the soils are estimated to expand the applicability of ACP.

2. Description of mobile devices

2.1 Automated dynamic cone penetrometer (ACP)

ACP is a portable in-situ penetration testing apparatus that characterizes the strength of the target ground. The ACP is composed of a cone tip with a diameter of 35.6 mm and an apex angle of 60°, an extendable driving rod with a diameter of 20 mm, and a drop hammer with a weight of 294.3 N, as shown in Fig. 1. The drop hammer is lifted using a hydraulic motor to a drop height of 200 mm; thus, the cone tip of the ACP dynamically penetrates the target ground with a potential energy of 58.86 N·m. The N-value of ACP (N_{ACP}) is obtained via the experimental results for ACP. N_{ACP}, which is blow count of the dropped hammer required for a penetration depth of 100 mm, is calculated as

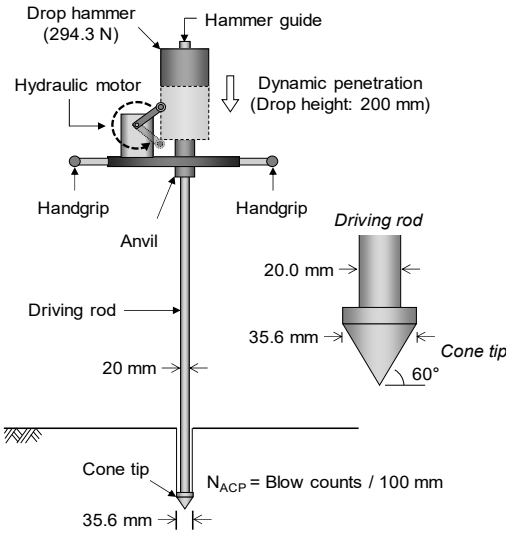

Fig. 1 Automated dynamic cone penetrometer (ACP)

$$N_{ACP}\left[blow\frac{counts}{100}mm\right] = N_{(D+100)mm} - N_{(D)mm} \quad (1)$$

where $N_{(D+100)mm}$ and $N_{(D)mm}$ are the cumulative blow counts of the hammer at the depths of (D + 100) mm and (D) mm, respectively. It should be noted that N_{ACP} is obtained by applying a permanent displacement to the target ground; thus, it can be used for the strength characterization of the target ground, similar to the N-value of the SPT.

The ACP can be carried and operated via manpower and characterizes the target ground at relatively greater depths owing to its automated hammer blowing system employing a hydraulic motor. Therefore, studies on the relationships between the N_{ACP} and other engineering properties are required for effective in-situ investigations using an ACP.

2.2 Dynamic cone penetrometer (DCP)

The conventional DCP, introduced by Scala (1956), is a miniaturized in-situ penetrometer. The components of the DCP are simpler than those of ACP: a cone tip with a diameter of 20 mm and an apex angle of 60°, a driving rod with a diameter of 16 mm, and a drop hammer with a weight of 78.5 N (ASTM D6951 2009), as shown in Fig. 2. The drop hammer is manually lifted and freely falls from a drop height of 575 mm, and the cone tip dynamically penetrates the target ground with a potential energy of 45.14 N·m. During penetration, blow counts and corresponding penetration depths of the cone tip are recorded to calculate the penetration depth at each hammer blow, which is defined as the DCPI (mm/blow).

$$DCPI[mm/blow] = D_{n+1} - D_n \quad (2)$$

where D_{n+1} and D_n are the depth of the cone tip at the blow

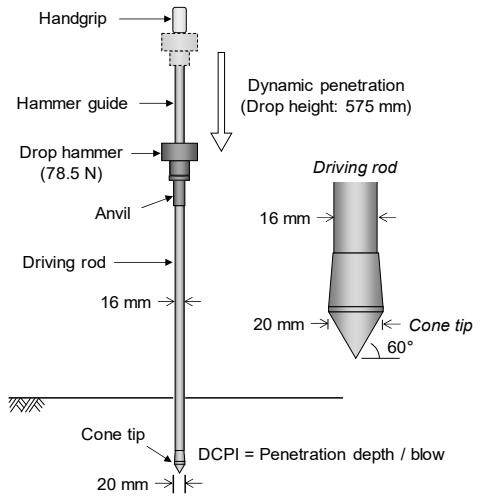

Fig. 2 Dynamic cone penetrometer (DCP)

counts of n+1 and n, respectively.

Owing to the simple testing procedure and equipment of DCP, the relationships between the DCPI and other engineering parameters such as relative density, internal friction angle, and elastic moduli have been investigated by several researchers for a wide range of applications of DCP (Lee *et al*. 2014, McElvaney and Bundadidjatnika 1991, Mohammadi *et al*. 2008). Accordingly, the DCP has been adopted as a standard instrument for managing and evaluating compacted subgrades during and after the construction of transportation infrastructures. However, because of the hand-operated hammer blowing system and low driving energy, the DCP is limited to characterizing target grounds at a shallow depth.

2.3 Light falling weight deflectometer (*LFWD*)

Even though the ACP and DCP offer significant advantages in that they are portable and characterize the target ground with depth, these approaches only determine the strength parameters. To evaluate the stiffness of the target ground, LFWD is being employed. The LFWD is a portable device that evaluates stiffness by applying a dynamic load on the loading plate by dropping hammer with a weight of 98.1 or 147.2 N, as shown in Fig. 3.

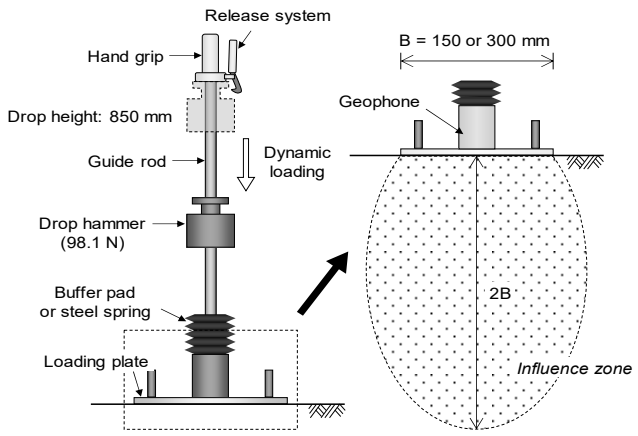

Fig. 3 Light falling weight deflectometer (LFWD)

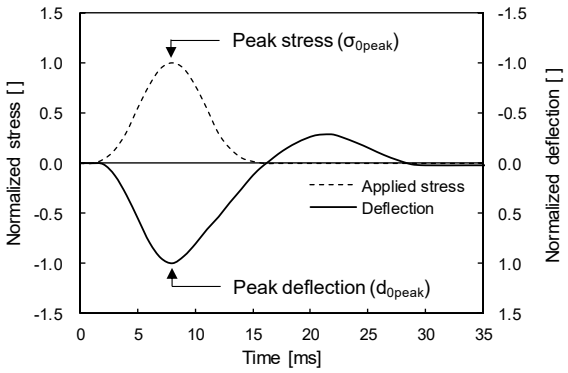

Fig. 4 Typical experimental result of light falling weight deflectometer (LFWD) test

When a dynamic load is applied on the loading plate, the plate is deflected; this deflection is measured in the time domain by using a geophone installed on the loading plate with the stress acting on the target ground, as shown in Fig. 4. The dynamic deflection modulus (E_{vd}), which is the elastic modulus evaluated via the LFWD test, is calculated using the peak stress acting on the target ground (σ_{0peak}) and the peak deflection of the loading plate (d_{0peak}), as follows

$$E_{vd}[MPa] = \frac{A \cdot (1-\nu^2) \cdot \sigma_{0peak} \cdot r}{d_{0peak}} \tag{3}$$

where A is the shape factor for stress distribution in the target ground, ν is Poisson's ratio, and r is the radius of the loading plate.

The LFWD evaluates E_{vd} within a short testing time and does not disturb the target ground; thus, the LFWD is highly applicable for the constructed geo-structures. However, the E_{vd} produced by LFWD is an equivalent modulus within the depth of the influence zone, which corresponds to twice the diameter (2B) of the loading plate (Elhakim *et al*. 2014, Fleming *et al*. 2007), as shown in Fig. 3. Accordingly, an error may occur if a discontinuity lies in the influence zone, and the ground deeper than the influence zone cannot be evaluated using the LFWD test.

3. Field tests

For the evaluation and comparison of N_{ACP}, DCPI, and E_{vd}, the ACP, DCP, and LFWD tests were conducted in the selected study sites. N_{ACP} and DCPI along the depth were compared to determine whether the strength indices indicate complementary results. In addition, E_{vd} evaluated by LFWD was compared with N_{ACP} to describe the consideration of the strain influence factor.

3.1 Site description

The ACP, DCP, and LFWD tests were carried out at three sites in South Korea, as shown in Fig. 5. Each site comprises three testing points; accordingly, the test results of nine points (Point-1 to 9) were compared. The testing points were determined by adopting soft ground that can undergo easy settling, resulting in engineering problems.

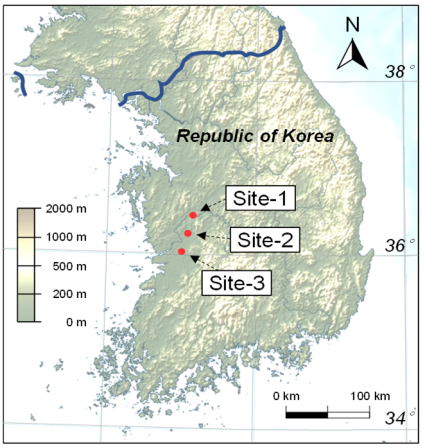

Fig. 5 Locations of field tests

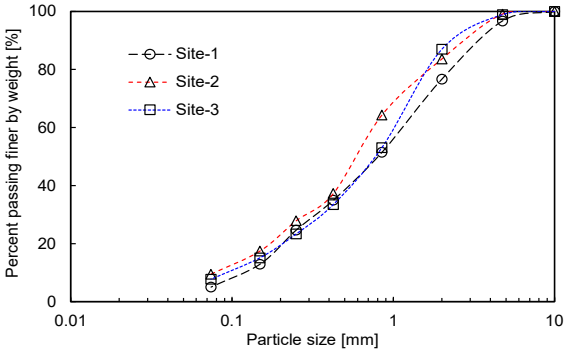

Fig. 6 Grain size distribution curves of samples

Table 1 Index properties of samples

Index property	Site		
	1	2	3
D_{10} [mm]	0.12	0.07	0.09
D_{30} [mm]	0.32	0.29	0.35
D_{50} [mm]	0.80	0.59	0.79
D_{60} [mm]	1.10	0.74	1.02
C_u [ ]	9.17	10.28	10.85
C_c [ ]	0.94	0.86	1.33
USCS [ ]	SP		SW

*D_n denotes grain size that corresponds to n% finer by weight. C_u, C_c, and USCS denote coefficient of uniformity, coefficient of curvature, and unified soil classification system, respectively

The representative grain size distribution curves of the samples from each site are shown in Fig. 6, and the index properties related to grain size characteristics are summarized in Table 1. At each testing point, the LFWD test was conducted to evaluate the soil stiffness of the in-situ ground before the disturbance that can be caused during the ACP and DCP tests. For the LFWD tests, a loading plate with a diameter of 300 mm was adopted, as shown in Fig. 7. Thereafter, ACP and DCP tests were performed until the hard ground layer emerged, or up to a depth of 10 m and 8 m, respectively. The spacing between the ACP and DCP

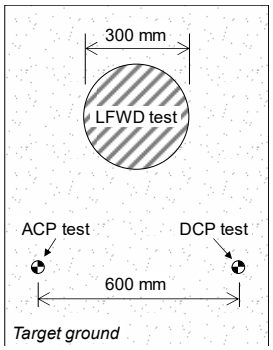

Fig. 7 Experimental setup on target ground

points was maintained at 600 mm to minimize the boundary effect of both penetration tests.

3.2 N-value (N_{ACP})

The values of N_{ACP} measured at Point-1 to Point-9 are presented in Fig. 8. The N_{ACP} at Point-1, 2, and 3 gradually increase along the depth because of the effective overburden pressure. At Point-2, the N_{ACP} abruptly increases at a depth of 2 m due to obstacles such as stone or gravel and returns to a gradually increasing line affected by the overburden pressure. The N_{ACP} values at Point-1 and 3 significantly increase beyond 60 blow counts/100 mm at the depth of 4.5 m when the hard ground layer emerges. At Point-4, 5, and 6, as shown in Fig. 8(b), N_{ACP} values gradually increase along the depth, but the effect of the overburden pressure was lower than that at Point-1, 2, and 3. The N_{ACP} at Point-6 abruptly increases up to 40 blow counts/100 mm at a depth of 0.5 m, similar to that for a depth of 2 m at Point-2. In contrast, the N_{ACP} at Point-7, 8, and 9 repeatedly increased and decreased along the depth up to 2 m because of naturally existing roots and gravels. Beyond a depth of 2 m, the ACP test is ceased because extremely soft and hard ground layers were noted at a depth of 2 m at Point-7 and 3.5 m at Point-8.

3.3 Dynamic cone penetration index (*DCPI*)

The DCPIs obtained at Point-1 to Point-9 at each site are plotted in Fig. 9. The low confining pressure near the ground surface induces large DCPIs for all tests. Note that a large DCPI corresponds to a low N_{ACP} due to the inverse units of [mm/blow] and [blow counts/100 mm]. Therefore, the DCPI profile shows more fluctuation as the resolution of DCPI is higher than that of N_{ACP}, where the measuring interval is fixed at 100 mm. In addition, the smaller diameter of DCP compared to that of ACP induces a more fluctuating profile due to the influence of relatively small particles (Bałachowski 2007). At Point-1 and 2, the DCPIs gradually decrease along the depth owing to the effective overburden pressure as indicated in the ACP result, and converge at 5 mm/blow and 7 mm/blow, respectively. At Point-3, the DCPI shows a relatively low value compared to that at Point-1 and 2, which corresponds to the result of ACP (see Fig. 8(a)). The DCPIs at Point-4, 5, and 6 gradually decrease along the depth, but the DCPIs converge

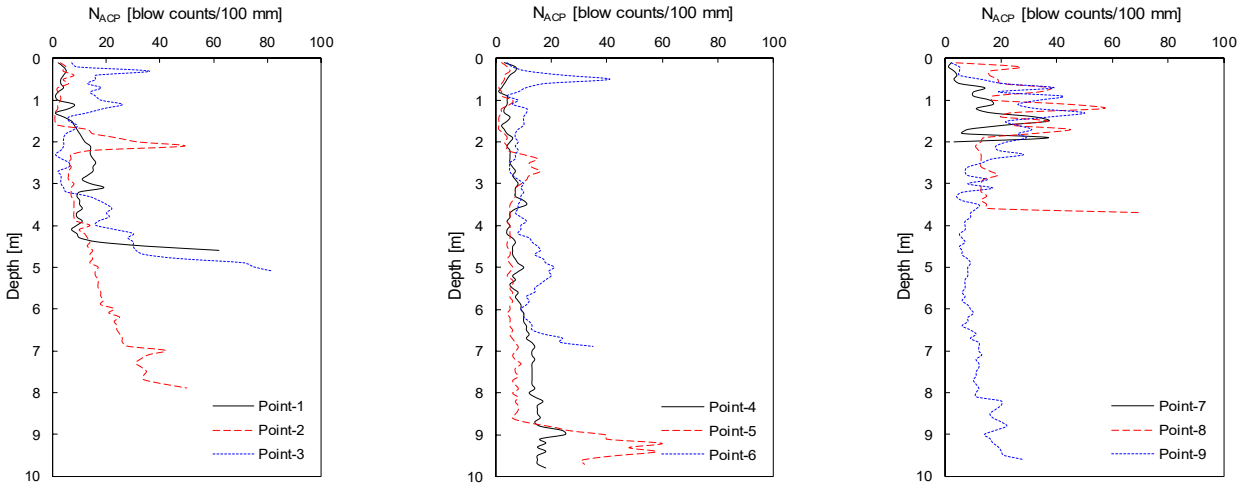

(a) Point-1, 2, 3 (b) Point-4, 5, 6 (c) Point-7, 8, 9

Fig. 8 Experimental results of automated dynamic cone penetration tests

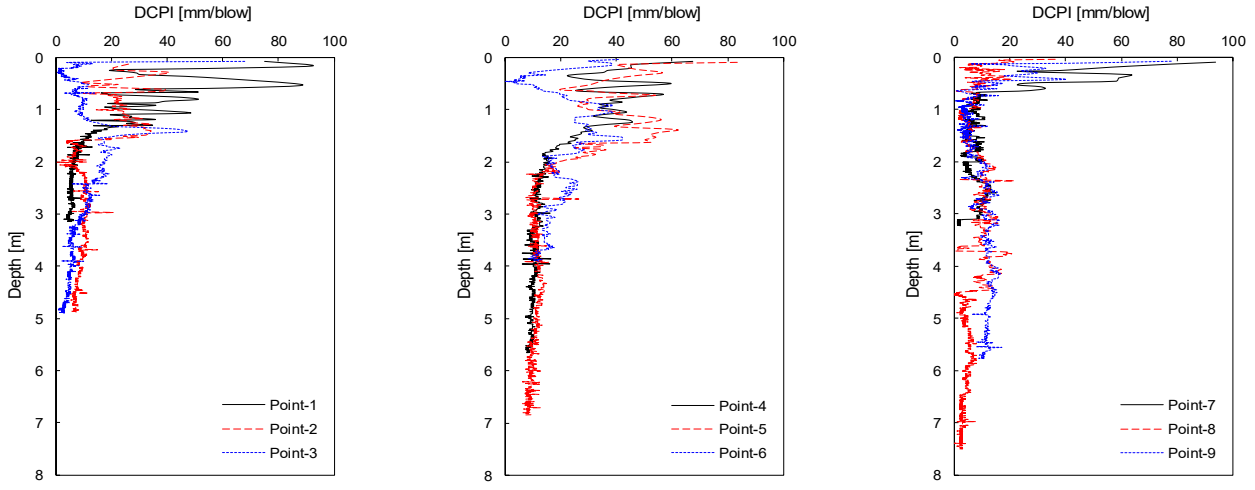

(a) Point-1, 2, 3 (b) Point-4, 5, 6 (c) Point-7, 8, 9

Fig. 9 Experimental results of dynamic cone penetration tests

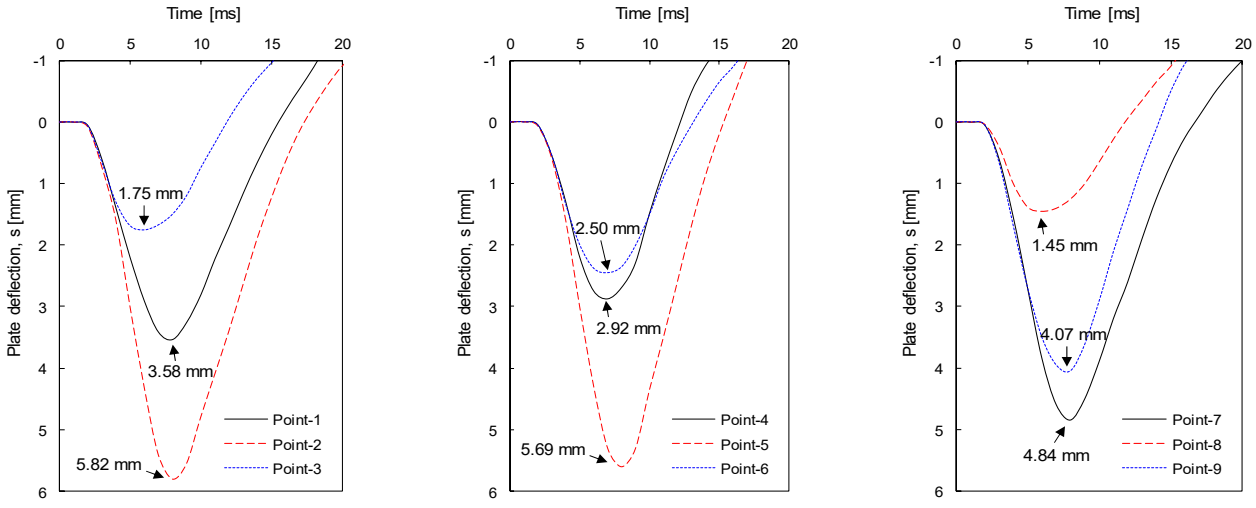

(a) Point-1, 2, 3 (b) Point-4, 5, 6 (c) Point-7, 8, 9

Fig. 10 Experimental results of light falling weight deflectometer tests

Table 2 Dynamic deflection modulus (E_{vd}) obtained using light falling weight deflectometer (LFWD)

Testing point	1	2	3	4	5	6	7	8	9
E_{vd} [MPa]	6.3	3.9	12.8	7.7	4.0	9.0	4.6	15.5	5.5

at 10–12 mm/blow, which is greater than those at Point-1, 2, and 3 owing to the smaller effective overburden pressure. In particular, the DCPI at a depth of 0.5 m at Point-6 reveals obstacles in the ground layer, which corresponds to the ACP result (see Fig. 8(b)). The DCPI at Point-7 is measured to be 5–10 mm/blow at depths of 0.8–2 m and 8–15 mm/blow at 2.5–3 m. Meanwhile, the DCPI at Point-8 is evenly measured to be 5–20 mm/blow from the ground surface to a depth of 7.5 m, and the DCPI at Point-9 is measured to be 2–18 mm/blow at a depth of 0.5–2 m. From the ground surface to a depth of 2 m, the DCPIs at Point-7, 8, and 9 show lower values compared to the other points due to the roots and gravels, which is in-line with the ACP results.

3.4 Dynamic deflection modulus (E_{vd})

The deflection curves resulting from the impulse load obtained using the LFWD for all testing points are presented in Fig. 10. Prior to the LFWD test, the ground surface was cleaned and smoothened without any protruding materials to ensure uniform contact between the loading plate and ground surface. The LFWD test is performed for at least three falling weight sequences, and the dynamic deflection modulus (E_{vd}) is measured unless the difference is greater than 3% (ASTM E2583 2007). The peak deflections generated by the impulse load at Point-1 to Point-9 are 3.58, 5.82, 1.75, 2.92, 5.69, 2.50, 4.84, 1.45, and 4.07 mm, respectively. E_{vd} values estimated by substituting the measured peak deflection in Eq. (3) are 6.3, 3.9, 12.8, 7.7, 4.0, 9.0, 4.6, 15.5, and 5.5, as summarized in Table 2.

4. Analyses and discussion

4.1 Correlations of N_{ACP} with DCPI and N_{DCP}

The DCPI has been widely used for the strength characterization of target ground and correlated with several engineering properties of soils such as relative density, internal friction angle, and elastic moduli (Hong *et al*. 2017, Lee *et al*. 2014, Mohammadi *et al*. 2008). Thus, the relationship between the DCPI and N_{ACP} was constructed to extend the applicability of N_{ACP}. To correlate the DCPI with N_{ACP}, the DCPI was averaged at depths of every 100 mm, and the averaged DCPI and N_{ACP} at corresponding depths are plotted in Fig. 11. The DCPI was fitted as a function of N_{ACP}, as follows

$$DCPI = 128.24 {N_{ACP}}^{-1} \quad (4)$$

In addition, the cumulative blow counts of DCP at depths of 100 mm (N_{DCP}) were calculated to verify the relationship between the DCPI and N_{ACP} (Eq. (4)) in identical dimension. The calculated N_{DCP} is linearly

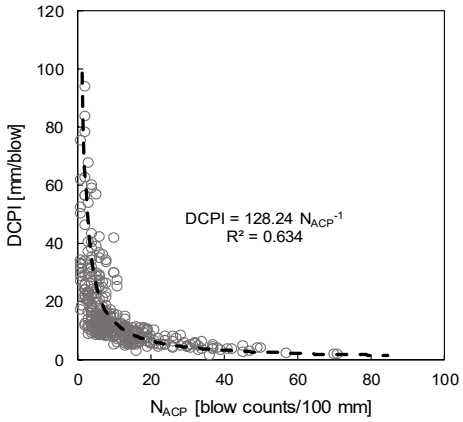

(a) Linear scale

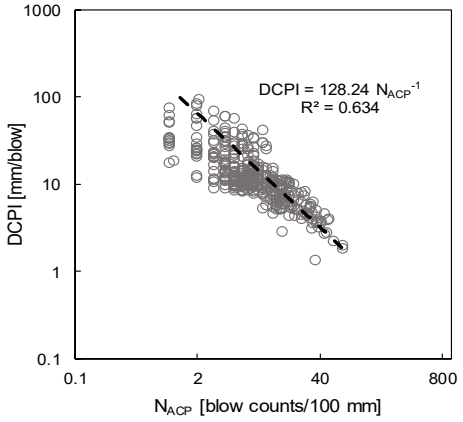

(b) Logarithmic scale

Fig. 11 Relationship between N_{ACP} and DCPI

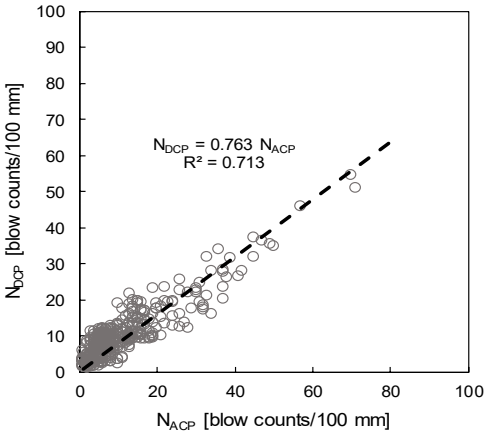

Fig. 12 Relationship between N_{ACP} and N_{DCP}

proportional to N_{ACP}, as shown in Fig. 12. Therefore, the relationship between the DCPI and N_{ACP} is considered as a valid equation and can be used for the estimation of DCPI from the results of the ACP tests.

4.2 Estimation of strength parameters using N_{ACP}

Both N_{ACP} and DCPI are not strength parameters but indices that characterize the strength of the target ground. For assessing the strength parameters of engineered soils

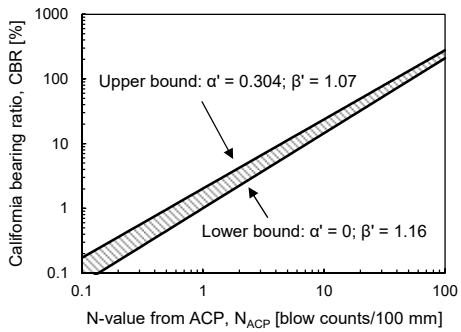

(a) California bearing ratio (CBR)

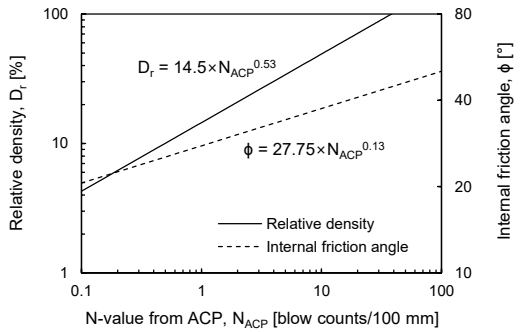

(b) Relative density (D_r) and internal friction angle (ϕ)

Fig. 13 Estimation of strength parameters using N_{ACP}

and pavements, the CBR, relative density (D_r), and internal friction angle (ϕ) are evaluated (Lee *et al*. 2019). To estimate the CBR using the portable penetration testing method, several researchers have suggested the following relationship between the logarithmic CBR and DCPI

$$log(CBR) = \alpha - \beta\, log(DCPI) \tag{5}$$

where α and β are correlation factors ranging from 2.44 to 2.56 and 1.07 to 1.16, respectively, according to the material characteristics of pavements (Harison 1987, Kleyn 1975, Livneh 1989, Livneh *et al*. 1995, McElvaney and Djatnika 1991, Webster *et al*. 1992). In addition, the relative density (D_r) and internal friction angle (ϕ) are correlated with the power of the DCPI, as follows

$$D_r, \phi = \frac{a}{DCPI^b} \tag{6}$$

where a and b are equal to 189.93 and 0.53 for D_r and 52.16 and 0.13 for ϕ (Mohammadi *et al*. 2008), respectively.

To estimate the CBR based on N_{ACP}, the relationship between the DCPI and N_{ACP} (Eq. (4)) is applied to Eq. (5); thus, the CBR can be estimated from N_{ACP}, as follows

$$\log(CBR) = \alpha' + \beta' \log(N_{ACP}) \tag{7}$$

where α' and β' are correlation factors ranging from 0 to 0.304 and 1.07 to 1.16, respectively. It should be noted that α' is determined by both α and β in Eq. (5) and that β' is identical to β in Eq. (5). The relationship between CBR and N_{ACP} is plotted in Fig. 13(a). The upper and lower bounds of the CBR are determined, where α' and β' are 0.304 and 1.07 and 0 and 1.16, respectively. In addition, the relationship between the DCPI and N_{ACP} (Eq. (4)) is substituted in Eq. (6) to estimate the relative density (D_r) and internal friction angle (ϕ) based on the N_{ACP}. D_r and ϕ can be estimated from N_{ACP} using Eq. (8) and Eq. (9), respectively, and these parameters are plotted on a logarithmic scale in Fig. 13(b).

$$D_r = 14.5{N_{ACP}}^{0.53} \tag{8}$$

$$\phi = 27.75{N_{ACP}}^{0.13} \tag{9}$$

Therefore, N_{ACP} can be used for the simple estimation of strength parameters such as CBR, D_r, and ϕ by using Eq. (7)-(9).

4.3 Correlations of E_{vd} with N_{ACP} and weighted N_{ACP}

The elastic modulus of the ground is one of the most important engineering parameters and can be used for evaluating the stiffness of the target ground. In this section, the relationship between the dynamic deflection modulus (E_{vd}) determined by LFWD tests and N_{ACP} was investigated to estimate the stiffness characteristics of the ground based on results of the ACP tests. For the comparison of E_{vd} and N_{ACP}, the N_{ACP} values measured to a depth of 600 mm were averaged ($N_{ACP\,(averaged)}$), which corresponds to the influence zone (2B) of the LFWD loading plate, and plotted with E_{vd}, as shown in Fig. 14. The relationship between E_{vd} and N_{ACP} is expressed as

$$E_{vd} = 0.547N_{ACP(averaged)} + 2.928 \tag{10}$$

Although E_{vd} is linearly correlated with N_{ACP}, the data sets are dispersed from the linear fitting line, and the determinant coefficient (R^2) is calculated to have a relatively small value of 0.715, because the LFWD evaluates an equivalent elastic modulus without considering the different strain levels within the influence zone.

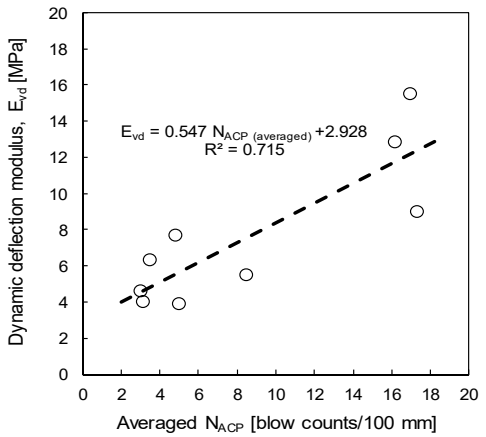

Fig. 14 Relationship between averaged N_{ACP} and dynamic deflection modulus (E_{vd})

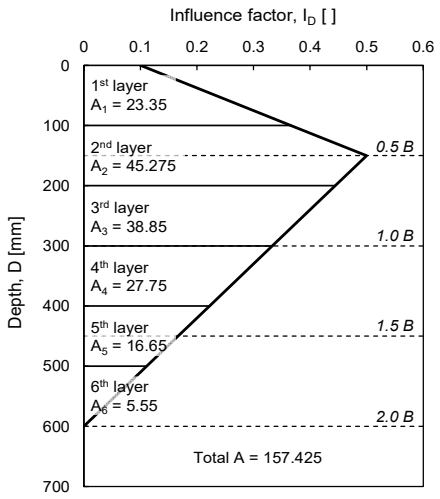

Fig. 15 Strain influence factor induced by LFWD test

To establish a reasonable relationship between E_{vd} and N_{ACP} while considering the strain levels induced by the LFWD test, a method for the estimation of the strain influence factor, suggested by Schmertmann *et al*. (1978), was adopted. The strain influence factor linearly increases from the surface and reaches a peak value at a depth corresponding to 0.5 B (150 mm); moreover, this factor linearly decreases to 0 at the depth of 2.0 B (600 mm), as shown in Fig. 15.

Based on the area of the strain influence factor, the weighting factors for depths of every 100 mm are calculated as

$$W_n = \frac{A_n}{\sum_{x=1}^{6} A_x} = \frac{A_n}{157.425} \tag{11}$$

where W_n and A_n are the weighting factor and area of the strain influence factor curve at the n-th layer, respectively. In addition, the weighted N_{ACP} ($N_{ACP(weighted)}$) was calculated as

$$N_{ACP(weighted)} = \sum_{x=1}^{6} N_{ACP(n)} \times W_n \tag{12}$$

where $N_{ACP(n)}$ is the N_{ACP} value at the n-th layer. $N_{ACP(weighted)}$ is plotted with E_{vd} in Fig. 16; $N_{ACP(weighted)}$ exhibits an improved linear relationship with E_{vd}, with a determinant coefficient of 0.927. E_{vd} is calculated using $N_{ACP(weighted)}$ as

$$E_{vd} = 0.887 N_{ACP(weighted)} + 2.114 \tag{13}$$

Therefore, the dynamic deflection modulus (E_{vd}) can be estimated using Eq. (13), and the stiffness of the target ground can be characterized along the depth based on the results of the ACP tests.

4.4 Estimation of stiffness parameters using N_{ACP}

For estimating the stiffness parameters of the target ground, elastic moduli were evaluated via the plate loading test (PLT), soil stiffness gauge (SSG), and falling weight deflectometer (FWD). Similar to the estimation of strength parameters in Eqs. (5) and (6), the elastic moduli determined via PLT (E_{PLT}), SSG (E_{SSG}), and FWD (E_{FWD}) are correlated with DCPI, as follows

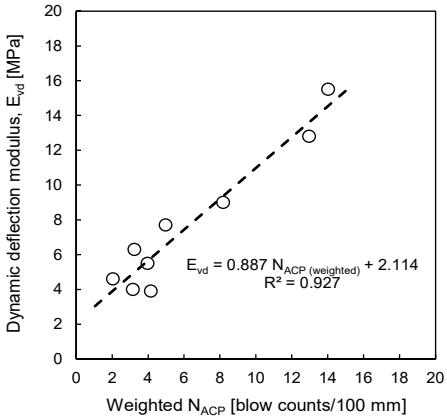

Fig. 16 Relationship between weighted N_{ACP} and dynamic deflection modulus (E_{vd})

$$E_{PLT}, E_{SSG}, E_{FWD} = \frac{c}{DCPI^d} \tag{14}$$

where c and d are 2460 and 1.285 for E_{PLT}, 755.2 and 0.671 for E_{SSG} (Alshibli *et al*. 2005), and 338 and 0.39 for E_{FWD} (Sawangsuriya and Edil 2005), respectively.

To assess the stiffness characteristics of the target ground using N_{ACP}, the relationships between the DCPI and N_{ACP} (Eq. (4)) are applied to Eq. (14). Thereafter, the relationships between the elastic moduli determined from the PLT (E_{PLT}), SSG (E_{SSG}), and FWD (E_{FWD}) and the N_{ACP} were constructed as shown in Fig. 17. E_{PLT}, E_{SSG}, and E_{FWD} are calculated using N_{ACP}, as follows

$$E_{PLT} = 4.81 {N_{ACP}}^{1.285} \tag{15}$$

$$E_{SSG} = 29.1 {N_{ACP}}^{0.671} \tag{16}$$

$$E_{FWD} = 50.9 {N_{ACP}}^{0.39} \tag{17}$$

Therefore, N_{ACP} can be used for the simple estimation of stiffness parameters such as E_{PLT}, E_{SSG}, and E_{FWD} by using Eqs. (15)-(17).

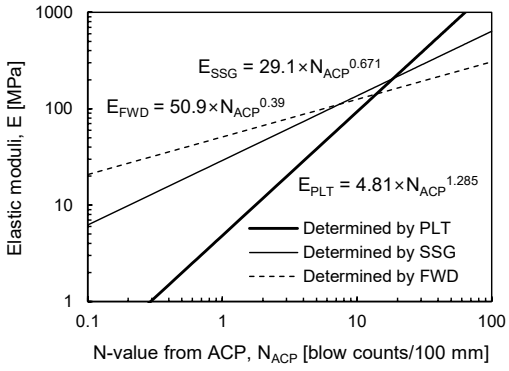

Fig. 17 Estimation of elastic moduli via PLT, SSG, and FWD using N_{ACP}

5. Conclusions

The objective of this study was to evaluate the engineering properties of subgrades using portable in-situ devices—the ACP, DCP, and LFWD—and to estimate engineering parameters based on the results of the ACP, DCP, and LFWD tests. These tests were conducted at nine testing points in South Korea. Based on the results of the ACP, DCP, and LFWD tests, the values of N_{ACP}, DCPI, and E_{vd} were evaluated. In addition, the relationships between N_{ACP} and the strength and stiffness parameters, i.e., the CBR, relative density (D_r), internal friction angle (ϕ), and elastic moduli determined by the PLT, SSG, and FWD, were constructed to efficiently evaluate the subgrade conditions based on N_{ACP}. The remarkable conclusions are as follows:

- The DCPI has been widely used and correlated with a number of engineering parameters owing to the simple procedure and equipment of the DCP test. Meanwhile, N_{ACP} can more effectively reflect the in-situ subgrade, because the ACP can rapidly characterize the deep layer owing to the automated hammer system. In addition, the portable LFWD can easily estimate the stiffness of the subgrade; however, the strain influence factor should also be considered.
- For an effective investigation of the in-situ subgrade, the value of N_{ACP} from the ACP test is correlated with the values of the DCPI and E_{vd} from the DCP and LFWD tests, respectively. The relationship between the DCPI and N_{ACP} is valid and suitable for the estimation of the DCPI, which is widely correlated with numerous engineering parameters. The correlation between E_{vd} and N_{ACP} improves when the strain influence factor is considered.
- To expand the applicability of ACP, the relationships between N_{ACP} and the strength and stiffness parameters, which are empirically and widely correlated with DCPI, are established. The CBR, D_r, ϕ, and elastic moduli determined via the PLT, SSG, and FWD are reliably estimated using N_{ACP}, proving that the N_{ACP} can be applied for the assessment of engineering parameters by using the correlations determined in this study.

Acknowledgments

This work was supported by the Gachon University research fund of 2019 (GCU-2019-0806).

This research was supported by Basic Science Research Program through the National Research Foundation of Korea (NRF) funded by the Ministry of Education (NRF-2018R1D1A1B07048182).

References

Alshibli, K.A., Abu-Farsakh, M. and Seyman, E. (2005), "Laboratory evaluation of the geogauge and light falling weight deflectometer as construction control tools", *J. Mater. Civil Eng.*, **17**(5), 560-569. https://doi.org/10.1061/(asce)0899-1561(2005)17:5(560)

ASTM D6951 (2009), Standard Test Method for Use of the Dynamic Cone Penetrometer in Shallow Pavement Applications, Annual Book of ASTM Standard, 04.03, ASTM International, West Conshohocken, PA, USA. https://doi.org/10.1520/d6951_d6951m

ASTM E2583 (2007), Standard Test Method for Measuring Deflections with a Light Weight Deflectometer, Annual Book of ASTM Standard, ASTM International, West Conshohocken, PA, USA. https://doi.org/10.1520/e2583-07

Bałachowski, L. (2007), "Size effect in centrifuge cone penetration tests", *Arch. Hydro-Eng. Environ. Mech.*, **54**(3), 161-181.

Briaud, J.L. (2013), *Geotechnical Engineering: Unsaturated and Saturated Soils*, John Wiley & Sons. https://doi.org/10.1002/9781118686195

Byun, Y.H. and Kim, D.J. (2020), "In-situ modulus detector for subgrade characterization", *Int. J. Pavement. Eng.* [Online published] https://doi.org/10.1080/10298436.2020.1743291

Byun, Y.H. and Lee, J.S. (2013), "Instrumented dynamic cone penetrometer corrected with transferred energy into a cone tip: a laboratory study", *Geotech. Test. J.*, **36**(4), 533-542. https://doi.org/10.1520/GTJ20120115

Chen, D.H., Lin, D.F., Liau, P.H. and Bilyeu, J. (2005), "A correlation between dynamic cone penetrometer values and pavement layer moduli", *Geotech. Test. J.*, **28**(1), 42-49. https://doi.org/10.1520/gtj12312

Elhakim, A.F., Elbaz, K. and Amer, M.I. (2014), "The use of light weight deflectometer for in situ evaluation of sand degree of compaction", *HBRC J.*, **10**(3), 298-307. https://doi.org/10.1016/j.hbrcj.2013.12.003

Farghaly, A.A. (2015), "Seismic analysis of 3-D two adjacent buildings connected by viscous dampers with effect of underneath different soil kinds", *Smart Struct. Syst., Int. J.*, **15**(5), 1293-1309. https://doi.org/10.12989/sss.2015.15.5.1293

Fleming, P.R., Frost, M.W. and Lambert, J.P. (2007), "Review of lightweight deflectometer for routine in situ assessment of pavement material stiffness", *Transport. Res. Rec.*, **2004**(1), 80-87. https://doi.org/10.3141/2004-09

Gabr, M.A., Hopkins, K., Coonse, J. and Hearne, T. (2000), "DCP criteria for performance evaluation of pavement layers", *J. Perform. Constr. Facil.*, **14**(4), 141-148. https://doi.org/10.1061/(asce)0887-3828(2000)14:4(141)

George, V., Rao, N.C. and Shivashankar, R. (2009), "PFWD, DCP and CBR correlations for evaluation of lateritic subgrades", *Int. J. Pavement Eng.*, **10**(3), 189-199. https://doi.org/10.1080/10298430802342765

Gidigasu, M.D. (1980), "Geotechnical evaluation of residual gravels in pavement construction", *Eng. Geol.*, **15**(3-4), 173-194. https://doi.org/10.1016/0013-7952(80)90033-2

Harison, J.A. (1987), "Correlation between California bearing ratio and dynamic cone penetrometer strength measurement of soils", *Proc. Inst. Civil Eng.*, **83**(4), 833-844. https://doi.org/10.1680/iicep.1987.204

Harison, J.A. (1989), "In situ CBR determination by DCP testing using a laboratory-based correlation", *Aust. Road Res.*, **19**(4), 313-317.

Hong, W.T., Byun, Y.H., Kim, S.Y. and Lee, J.S. (2016), "Cone penetrometer incorporated with dynamic cone penetration method for investigation of track substructures", *Smart Struct. Syst., Int. J.*, **18**(2), 197-216. https://doi.org/10.12989/sss.2016.18.2.197

Hong, W.T., Kim, S.Y., Lee, S.J. and Lee, J.S. (2017), "Strength and stiffness assessment of railway track substructures using crosshole-type dynamic cone penetrometer", *Soil Dyn. Earthq. Eng.*, **100**, 88-97. https://doi.org/10.1016/j.soildyn.2017.05.021

Kim, S.Y. and Lee, J.S. (2020), "Energy correction of dynamic

cone penetration index for reliable evaluation of shear strength in frozen sand–silt mixtures", *Acta Geotech*., **15**(4), 947-961. https://doi.org/10.1007/s11440-019-00812-y

Kleyn, E.G. (1975), "The Use of the Dynamic Cone Penetrometer (DCP)", Transvaal Provincial Administration, Report No. 2/74, South Africa.

Kong, S.M., Kim, D.M., Lee, D.Y., Jung, H.S. and Lee, Y.J. (2018), "Field and laboratory assessment of ground subsidence induced by underground cavity under the sewer pipe", *Geomech*. *Eng*., *Int*. *J*., **16**(3), 285-293. https://doi.org/10.12989/gae.2018.16.3.285

Lee, J.S. and Byun, Y.H. (2020), "Instrumented Cone Penetrometer for Dense Layer Characterization", *Sensors*, **20**(20), 5782. https://doi.org/10.3390/s20205782

Lee, C., Kim, K.S., Woo, W. and Lee, W. (2014), "Soil stiffness gauge (SSG) and dynamic cone penetrometer (DCP) tests for estimating engineering properties of weathered sandy soils in Korea", *Eng*. *Geol*., **169**, 91-99. https://doi.org/10.1016/j.enggeo.2013.11.010

Lee, J.S., Kim, S.Y., Hong, W.T. and Byun, Y.H. (2019), "Assessing subgrade strength using an instrumented dynamic cone penetrometer", *Soils Found*., **59**(4), 930-941. https://doi.org/10.1016/j.sandf.2019.03.005

Livneh, M. (1989), "Validation of correlations between a number of penetration tests and in situ California bearing ratio tests", *Transport*. *Res*. *Rec*., **1219**, 56-67.

Livneh, M., Ishai, I. and Livneh, N.A. (1995), "Effect of vertical confinement on dynamic cone penetrometer strength values in pavement and subgrade evaluations", *Transport*. *Res*. *Rec*., **1473**, 1-8.

McElvaney, J. and Bundadidjatnika, I.R. (1991), "Strength evaluation of lime-stabilised pavement foundations using the dynamic cone penetrometer", *Aust*. *Road Res*., **21**(1), 45-52.

Mir, M., Bouafia, A., Rahmani, K., and Aouali, N. (2017), "Analysis of load-settlement behaviour of shallow foundations in saturated clays based on CPT and DPT tests", *Geomech*. *Eng*., *Int*. *J*., **13**(1), 119-139. https://doi.org/10.12989/gae.2017.13.1.119

Mohammadi, S.D., Nikoudel, M.R., Rahimi, H. and Khamehchiyan, M. (2008), "Application of the dynamic cone penetrometer (DCP) for determination of the engineering parameters of sandy soils", *Eng*. *Geol*., **101**(3-4), 195-203. https://doi.org/10.1016/j.enggeo.2008.05.006

Nazzal, M., Abu-Farsakh, M., Alshibli, K. and Mohammad, L. (2004), "Evaluating the potential use of a portable LFWD for characterizing pavement layers and subgrades", In: *Geotechnical Engineering for Transportation Projects*, *Proceedings of GeoTrans 2004*, Los Angeles, CA, USA, July, pp. 915-924. https://doi.org/10.1061/40744(154)79

Putri, E.E., Kameswara, N.S.V.R. and Mannan, M.A. (2012), "Evaluation of modulus of elasticity and modulus of subgrade reaction of soils using CBR test", *J*. *Civil Eng*. *Res*., **2**(1), 34-40. https://doi.org/10.5923/j.jce.20120201.05

Roy, S. (2016), "Assessment of soaked California bearing ratio value using geotechnical properties of soils", *Resour*. *Environ*., **6**(4), 80-87. https://doi.org/10.5923/j.re.20160604.03

Sawangsuriya, A. and Edil, T.B. (2005), "Evaluating stiffness and strength of pavement materials", *Proc*. *Inst*. *Civil Eng*. *Geotech*. *Eng*., **158**(4), 217-230. https://doi.org/10.1680/geng.2005.158.4.217

Scala, A.J. (1956), "Simple methods of flexible pavement design using cone penetrometers", *New Zeal*. *Eng*., **11**(2), 34-44.

Schmertmann, J.H., Brown, P.R. and Hartman, J.P. (1978), "Improved strain influence factor diagrams", *J*. *Geotech*. *Geoenviron*. *Eng*., **104**(8), 1131-1135. https://doi.org/10.1061/AJGEB6.0000683

Sujatha, E.R., Geetha, A.R., Jananee, R. and Karunya, S.R. (2018), "Strength and mechanical behaviour of coir reinforced lime stabilized soil", *Geomech*. *Eng*., *Int*. *J*., **16**(6), 627-634. https://doi.org/10.12989/gae.2018.16.6.627

Usluogullari, O.F. and Vipulanandan, C. (2011), "Stress-strain behavior and California bearing ratio of artificially cemented sand", *J*. *Test*. *Eval*., **39**(4), 637-645. https://doi.org/10.1520/jte103165

Webster, S.L., Grau, R.H. and Williams, T.P. (1992), "Description and application of dual mass dynamic cone penetrometer", U.S. Army Corps of Engineers Waterways Experiment Station, Vicksburg. Instruction Report GL-92-3.

HJ